



Article

Enzymatic Treatment of Ferulated Arabinoxylans from Distillers Dried Grains with Solubles: Influence on the Fabrication of Covalent Electro-Sprayed Nanoparticles

Yubia De Anda-Flores ^{1,*}, Jaime Lizardi-Mendoza ¹, Agustín Rascón-Chu ², Judith Tanori-Cordova ³, Ana Luisa Martínez-López ⁴ and Elizabeth Carvajal-Millan ^{1,*}

¹ Biopolymers-CTAOA, Research Center for Food and Development (CIAD, A.C.), Carretera Gustavo Enrique Astiazarán Rosas No. 46, Hermosillo 83304, Mexico; jalim@ciad.mx

² Biotechnology-CTAOV, Research Center for Food and Development (CIAD, A.C.), Carretera Gustavo Enrique Astiazarán Rosas No. 46, Hermosillo 83304, Mexico; arascon@ciad.mx

³ Department of Polymers and Materials Research, University of Sonora, Hermosillo 83000, Mexico; jtanori@unison.mx

⁴ NANO-VAC Research Group, Department of Chemistry and Pharmaceutical Technology, University of Navarra, 31008 Pamplona, Spain; anluisa.mtz@gmail.com

* Correspondence: yubia.deanda@ciad.mx (Y.D.A.-F.); ecarvajal@ciad.mx (E.C.-M.); Tel./Fax: +52-(662)-289-2400 (ext. 603) (Y.D.A.-F. & E.C.-M.)



Citation: De Anda-Flores, Y.; Lizardi-Mendoza, J.; Rascón-Chu, A.; Tanori-Cordova, J.; Martínez-López, A.L.; Carvajal-Millan, E. Enzymatic Treatment of Ferulated Arabinoxylans from Distillers Dried Grains with Solubles: Influence on the Fabrication of Covalent Electro-Sprayed Nanoparticles. *Polysaccharides* **2023**, *4*, 358–370. <https://doi.org/10.3390/polysaccharides4040021>

Academic Editor: Florin Oancea

Received: 13 July 2023

Revised: 22 August 2023

Accepted: 8 September 2023

Published: 2 October 2023



Copyright: © 2023 by the authors. Licensee MDPI, Basel, Switzerland. This article is an open access article distributed under the terms and conditions of the Creative Commons Attribution (CC BY) license (<https://creativecommons.org/licenses/by/4.0/>).

Abstract: Arabinoxylans (AXs) extracted from distillers dried grains with solubles (DDGSs) were treated with amylase, amyloglucosidase, and protease, to evaluate their effect on the polysaccharide capability to form covalent electro-sprayed nanoparticles. Enzymatically treated arabinoxylans (AXPPs) presented a significant decrease in protein content and molecular weight (31 and 37%, respectively), while the ferulic acid content and the arabinose-to-xylose ratio (A/X) were not statistically modified. The Fourier transform infrared spectra of the AXPPs showed a diminution in the intensity of amide I and amide II bands concerning AXs. The AXPP gels (1% *w/v*) induced via laccase registered a slight increase in the dimers of ferulic acid cross-linking content (9%) and the G' value (27%) about the AX gels. The electro-sprayed nanoparticles of AXs and AXPPs (NAXs and NAXPPs, respectively) revealed a spherical and regular morphology via transmission electron microscopy. The nanoparticle diameter was not different for the NAXs and NAXPPs, while the NAXPPs show a significant reduction in Z potential value compared to NAXs. Confocal laser microscopy observations were conducted, to analyze the protein content in the AX network, and a decrease in illuminated areas was observed in the AXPP gels and the NAXPPs. These results indicate that the enzymatical treatment of an AX improves the polysaccharide gelling capability, but does not influence the fabrication of electro-sprayed covalent nanoparticles. NAXs and NAXPPs could be attractive biomaterials for diverse pharmaceutical and biomedical applications.

Keywords: arabinoxylans; enzymes; nanoparticles; biomaterial; biomedicine

1. Introduction

Arabinoxylans (AXs) are structural polysaccharides in the cell walls of different grains, such as maize, rice, sorghum, wheat, etc. Most AXs and other polymers are cross-linked with other components, such as cellulose microfibrils, via hydrogen bonds, which confer specific stability characteristics [1,2]. AXs can be recovered from maize by-products, such as distillers dried grains with solubles (DDGSs), through chemical or enzymatic treatment [3,4]. The chemical composition of DDGSs varies, according to the maize origin and bioethanol production [5]. Linear units of xyloses constitute an AX in a β -1,4 chain, and these units can be substituted by α -L-arabinofuranose ramifications in α -1, at the O-2 and/or O-3 positions. The arabinoses can be esterified by ferulic acid (FA) at the O-5 position. Usually, ferulic acid dimers (di-FAs) and trimers (tri-FAs) can be present in the AX chain [6,7]. The AXs can

form gels due to their FA content, via oxidizing enzymatic (laccase/peroxidase systems) or chemical (ferric chloride, ammonium persulfate) both oxidizing agents favor the new di-FA and tri-FA formation. The di-FAs detected in AX gels are 5-5', 8-5' benzo, 8-O-4', 8-5', and 8-8' isomers, and one tri-FA 4-O-8', 5-5' [8–12]. Additionally, the AX contains small amounts of protein associated with the AX chain (Figure 1) [13,14].

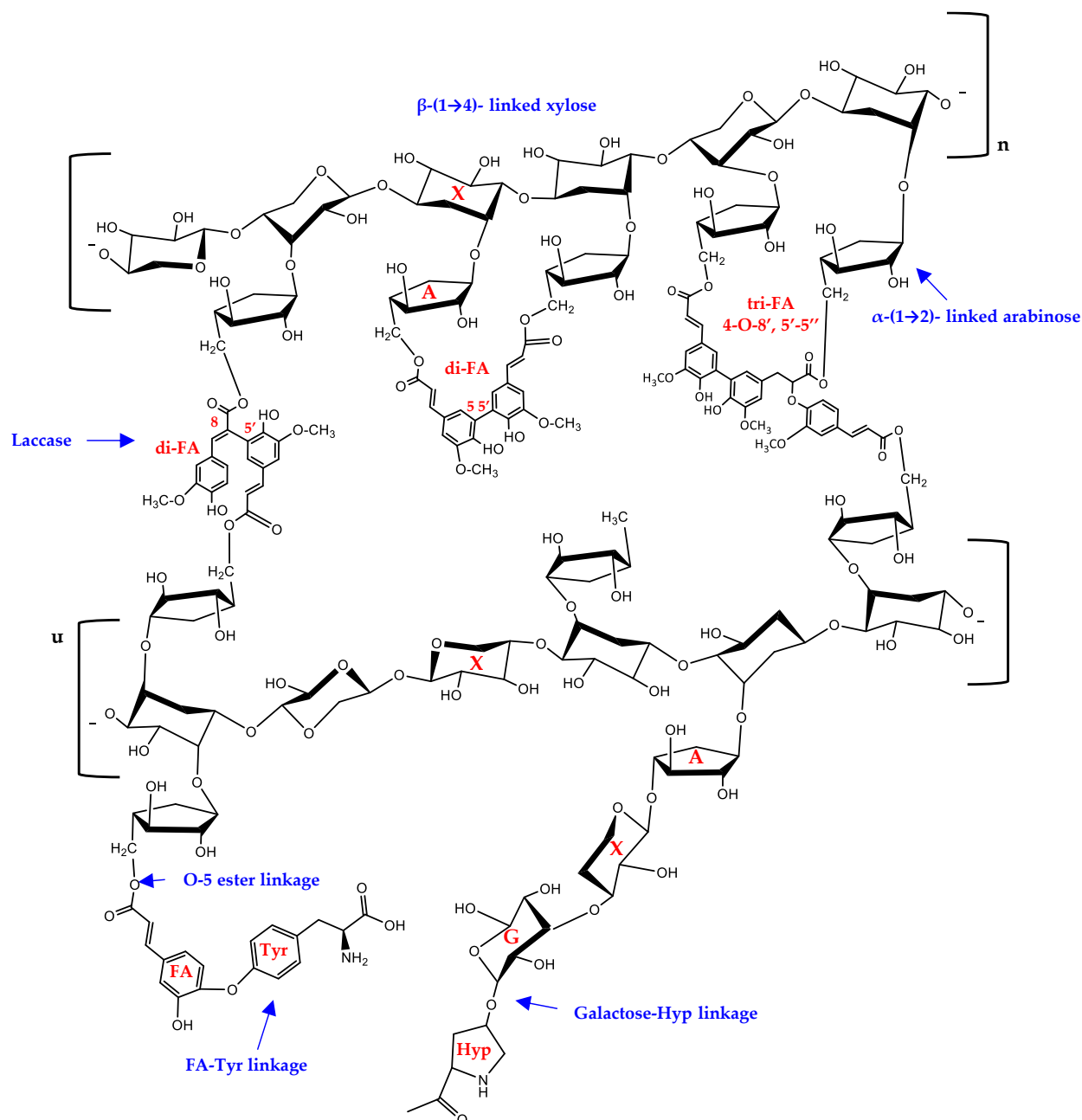


Figure 1. The main structure of arabinoxylan from DDGSs: A, arabinose; X, xylose; G, galactose; FA, ferulic acid; ferulic acid dimers (di-FAs, 8-5' and 5-5'), ferulic acid trimer (tri-FAs, 4-O-8', 5-5'); Tyr, tyrosine; Hyp, hydroxyproline.

The study of the AX structure is highly relevant when exploring new possibilities for its potential application. An important structural characteristic is the presence of a residual protein that is associated or strongly bound to the polysaccharide chain, which is not eliminated during the extraction and purification processes used to obtain the AX; besides, this characteristic can provide emulsifying properties to the polysaccharide [15].

Due to it not being possible to eliminate this residual protein, chemical and enzymatic modification assays have proven useful for reducing its presence, and achieving the purification of these polysaccharides [16,17]. In enzymatic treatments, the enzymes α -amylase and amyloglucosidase are used to remove any remaining starch and the presence of plant compounds, such as cellulose, which could have remained in the polysaccharide [18,19]. Additionally, the proteases participate in processes of degradative proteolysis, carrying out the broadest hydrolysis of the target proteins, which includes the cleavage of multiple peptide bonds and, ultimately, the complete conversion of the protein into amino acids [20].

A previous study [21] isolated and identified the protein from maize AXs. This protein presented a peptide sequence and molecular weight of 22 kDa. These authors suggested two association pathways between the AX chain and the protein. These pathways involve covalent-type bonds, which are still under study. They also propose that the protein can be covalently or physically bound to the structure of the AX, and suggest that the possible interaction between the AX and the protein is via the FA-amino acids bound through forming an AF-tyrosine dimer (Tyr). The other possible interaction is the union between the amino acid and carbohydrate, through a covalent bond that involves the union of the polysaccharide with the protein, through the amino acid hydroxyproline (Hyp). However, these proposals for possible links, though interesting, still need to be verified. A previous investigation reported histidine (HIS), threonine (Thr), and asparagine (Asn) as the primary amino acids in the protein associated with AXs extracted from DDGSs [22]. Significant amounts of protein have been found in AXs extracted from maize sources. A previous study reported partially removing this AX-associated protein from DDGSs, showing a 53% reduction after protease treatment [14]. The remaining protein remains attached, and few advances have been reported in terms of stripping the AX from the protein completely.

The AX can form gels in the presence of an oxidative agent [12], depending on the AX structural characteristics, such as the FA content, arabinose/xylose ratio, and molecular weight [10]. The residual protein in the AX chain is another structural characteristic associated with gelling properties [23]. The AX matrices can encapsulate, entrap, and release biomacromolecules, such as insulin and probiotic bacteria, and potentially be used in various pharmaceutical and biomedical applications [24–27]. These matrices have become promising materials for drug delivery systems, due to their biocompatibility, biodegradability, and non-toxic properties [28]. The capability of AXs to form covalently cross-linked nanoparticles was recently reported [29]. However, that investigation did not consider the effect of the protein content on this polysaccharide's properties. This protein's presence could significantly confer properties in manufacturing nanoparticles, the extent of which is still under study.

The objective of the current study was to assess the impact of the partially enzymatic protein remotion of an AX on the formation and evaluation of the morphological characteristics of the covalently electro-sprayed nanoparticles derived from it.

2. Materials and Methods

2.1. Materials

AXs from DDGSs were obtained as previously reported [30]. Laccase (from *Trametes versicolor*, E.C.1.10.3.2), protease from *Bacillus licheniformis*, amyloglucosidase from *Aspergillus niger*, α -amylase from *Bacillus licheniformis* type XII-A, β -lactoglobulin from bovine milk, and the chemicals used were obtained from Sigma Aldrich Co. (St. Louis, MO, USA).

2.2. Enzymatic Treatment of AXs

The AXs were enzymatically treated and dialyzed. In brief, the AX solution (2% w/v) and the enzymes were prepared in 0.1 M acetate buffer (pH 6). The enzymes were added to the AX solution as follows: α -amylase (2800 U/g sample, 100 °C, 30 min, pH 6), amyloglucosidase (24 U/g polysaccharides, 3 h, 50 °C, pH 5), and protease (4 U/g polysaccharides, 16 h, 20 °C, pH 7.5, followed by boiling at 100 °C for 10 min). Then, the sample was centrifuged at 6000 rpm at 20 °C for 15 min. The supernatant was recovered and dia-

lyzed (Cellulose ester membrane, 6–8 kDa) at 25 °C for 22 h. The dialyzed solution was lyophilized, to obtain dry partially purified AX (AXPP) [14].

2.3. Phenolic Acid Analysis

The ferulic acid (FA), ferulic acid dimer (di-FA), and ferulic acid trimer (tri-FA) contents in the AX and AXPP powder and gel were quantified via high-performance liquid chromatography, as previously reported [31]. Briefly, 50 mg of AX and AXPP samples were saponified with 2 mL of 2 N NaOH, agitated at 100 rpm, and kept at 35 °C for 2 h in darkness. Subsequently, the pH was adjusted to 2.0, using 3,4,5-trimethoxycinnamic acid (TMCA) and 4 N hydrochloric acid. To recover the phenolic acids, 5 mL of diethyl ether was employed twice, followed by evaporation under nitrogen gas at 40 °C (Dri-Block DB-3A, Techne, UK). The resulting extract was reconstituted in 1 mL of methanol: water (50:50), and then filtered through a 0.45 µm (Millipore, St. Louis, MO, USA). The chromatographic separation of the phenolic acids was determined using an Alltima C18 column (250 × 4.6 mm; Alltech Associates, Inc., Deerfield, IL, USA). Detection was achieved via measuring the UV absorbance at 320 nm.

2.4. Protein Analysis

The protein quantification in the AX and AXPP was carried out according to the Bradford method [32]. The protein standard BSA (β -Lactoglobulin from bovine milk) was prepared from 0.1 to 1.4 mg/mL for the standard curve. Firstly, 1 mg of the AX and AXPP samples was diluted in 100 µL of water in a tube, then 3 mL of Bradford Reagent was added and vortexed gently. The samples were incubated at room temperature for 15 min. Then, the samples were transferred into cuvettes, and analyzed via absorbance at 595 nm using the Cary 60 UV-VIS Spectrophotometer (Agilent Technologies, Santa Clara, CA, USA).

2.5. Fourier Transform Infra-Red (FTIR) Spectroscopy

The FTIR spectra for the AX and AXPP samples were recorded using a Nicolet iS50 FTIR Spectrometer (Madison, WI, USA). The samples were placed on an ATR module, and the FTIR spectrum was analyzed in absorbance mode (4000–400 cm⁻¹) [4].

2.6. Macromolecular Characteristics

The macromolecular characteristics of the AX and AXPP were determined via the size-exclusion chromatography (SEC) system on a DAWN HELOS-II 8 multi-angle laser light-scattering (MALS) instrument detector, coupled with a ViscoStar-II Viscometer, and a refractive index (RI) Optilab T-rex detector (Wyatt Technology Corp., Santa Barbara, CA, USA), as previously reported [26]. Briefly, 5 mg of the samples was dissolved in 50 mM NaNO₃/0.02% NaN₃, and heated at 80 °C for 1 h. The solution was centrifuged (15,000 rpm for 10 min) and filtered (0.45 µm, Millipore, St. Louis, MO, USA). The results were analyzed and calculated using the software ASTRA 6.1 [33].

2.7. AX and AXPP Covalent Cross-Linking

The AX and AXPP solutions (1% *w/v*) and laccase solution (1.675 nkat/mg AX) were prepared in 0.1 M acetate buffer (pH 5.5). Laccase was used as an enzymatic cross-linking agent. The gelling formation was investigated using a small deformation oscillatory rheometer (Discovery HR-2, TA Instruments, New Castle, DE, USA). The samples were placed onto the rheometer's parallel-plate geometry (40 mm diameter) at 4 °C. The rheological properties were monitored at 0.25 Hz and 5% strain for 90 min at 25 °C. The mechanical (0.01–10 Hz) and strain (0.02–20%) spectra were recorded for the gel formed [13].

2.8. Nanoparticles Fabrication

AX nanoparticles (NAXs) and AXPP nanoparticles (NAXPPs) were obtained, as previously reported [29]. The coaxial electro-spray technique (Profector Life Science, Dublin, Ireland) was used [34]. The AX and AXPP dispersions (1% *w/v*) in 0.1 M acetate buffer

at pH 5.5 were used in the internal syringe, and the laccase dispersion (1.675 nkat/mg AX) in the outer syringe. The dispersions were injected at 1 mL/h, using two pumps (WorldPrecision Instruments, AL-1000, Sarasota, FL, USA). The NAXs and NAXPPs were recovered in mineral oil at 500 rpm for 24 h at 25 °C.

2.9. Dynamic Light Scattering (DLS) Analysis

The NAXs and NAXPPs were washed with ultrapure water (Milli-Q), vortexed (1 min), centrifuged (2000×*g*, 10 min, 20 °C), and then resuspended (0.3 mg/mL), and filtered through a 1.4 μm membrane before measurement. Then, the sample was loaded into a disposable quartz cell for DLS analysis. The size distribution and Z potential were registered using a Möbiuζ (Wyatt Technology Corp., Santa Barbara, CA, USA) at 532 nm, and a detection angle of 163.5° [29].

2.10. Transmission Electron Microscopy (TEM) Analysis

The NAXs and NAXPPs (9 μL) were resuspended on ultrapure water, deposited on a TEM grid (carbon-coated copper), and dried at room temperature (25 °C). Phosphotungstic acid was used for the negative staining of the sample. The morphology and size of the NAXs and NAXPPs were analyzed using a transmission electron microscope at 200 kV (JEM 2010F, JEOL, Ltd., Tokyo, Japan) [35].

2.11. Confocal Laser Scanning Microscopy (CLSM) Analysis

The AXs, AXPPs (1% *w/v*), and rhodamine B isothiocyanate (RICT) at 0.02% were dispersed in 0.1 M acetate buffer at pH 5.5. Then, gels were made up using laccase solution (1.675 nkat/mg AX), and the NAXs and NAXPPs were fabricated as mentioned above (2.8). The analysis was performed with a C2+ Confocal Microscope System (Nikon, Japan) in the fluorescent mode for RITC at 570 nm. The study was observed at 25 °C [13].

2.12. Statistical Analysis

Chemical analysis, rheological measurements, and nanoparticle characterization were performed in triplicate, and the results were expressed as mean and standard deviation. Statistical analysis was performed using Student's *t*-test, and the differences among means were compared via the Mann–Whitney U-test (*p* < 0.05).

3. Results and Discussion

3.1. AX and AXPP Characterization

The α-amylase, amyloglucosidase, and protease enzymes were used to purify the polysaccharide, and remove the protein associated with the AX chain. After enzymatic treatment, the AXPP presented a protein content of 11%, corresponding to a protein diminution of 31% compared to the AX (Table 1). The present protein content values are greater than those reported for AXs from DDGSs (8.2% in AXs before treatment, and 3.82% after treatment), which also presented a larger protein diminution (53%) [14]. In the current research, the AX's enzymatic treatment and dialysis did not affect its arabinose-to-xylose ratio (A/X) and FA content. The α-amylase and amyloglucosidase treatment allowed us to obtain a purer AX, by breaking down the covalent bonds between the glucose units in the starch [36]. However, after protease treatment, the AXPPs presented an increase of 51% in their total di-FA and tri-FA presence. The increase in the di-FA and tri-FA content following enzymatic treatment and dialysis can be attributed to their association with the high-molecular-weight chains of AXs. Consequently, subjecting AXs to enzymatic treatment and dialysis with a membrane of >50 kDa removes low-molecular-weight chains.

The A/X ratio for the AX and AXPP was 1.16 and 1.13, respectively, indicating a highly branched structure. The macromolecular characteristics of the AX and AXPP are also presented in Table 1. The molecular weight (Mw), intrinsic viscosity ([η]), polydispersity index (PI), and hydrodynamic radius (Rh) values were in the range reported for other AXs from DDGSs [30]. In a previous study [37], the enzymatic degradation of gum arabic was

carried out through treatment with proteases, in which it was observed that the samples treated for 24 h at a temperature of 37 °C exhibited a reduction in molecular weight. The researchers pointed out that the main effect of this enzymatic degradation is a decrease in the molecular weight of the gum arabic. In our study, the AXPP Mw presented a reduction of 37%, and there was a slight increase in $[\eta]$ compared to the AX, indicating a conformational change after enzymatic treatment (Table 1).

Table 1. The composition and macromolecular characteristics of the AX and AXPP.

	AX	AXPP
Protein (% p/p)	16 ± 0.05 ^a	11 ± 0.12 ^b
A/X ratio	1.16 ± 0.08 ^a	1.13 ± 0.01 ^a
* Ferulic acid (FA)	7.3 ± 0.2 ^a	7.3 ± 0.2 ^a
* Dimers of FA (di-FAs)	0.212 ± 0.009 ^b	0.32 ± 0.07 ^a
* Trimers of FA (tri-FAs)	traces	0.06 ± 0.02
+ Molecular weight (Mw) (kDa)	661	420
+ Intrinsic viscosity $[\eta]$ (mL/g)	149	165
+ Polydispersity index (PI) (Mw/Mn)	2.4	2.0
+ Radius of gyration RG (nm)	40	37
+ Hydrodynamic radius Rh (nm)	22.5	20.0
+ Characteristic ratio (C_∞)	14.2	18.6
+ q (nm)	4.1	5.3
+ Mark–Houwink–Sakurada α	0.536	0.607
+ Mark–Houwink–Sakurada K (mL/g)	1.394 × 10 ⁻¹	7.804 × 10 ⁻²

* Results expressed in $\mu\text{g}/\text{mg}$ polysaccharide. + Absolute values. The mean value of triplicate determinations ± SD. Values with similar letters in a column do not differ significantly ($p < 0.05$). q: persistence length (calculated based on unbranched arabinoxylans).

Complementarily, the molecular identity was also explored. The FTIR spectrum of the AX and AXPP are presented in Figure 2. Both spectra showed the absorbance region between 1200 and 800 cm^{-1} , representing the particular AX region [38,39]. The absorption bands detected at the 1030 cm^{-1} and 907 cm^{-1} signals are related to the C-OH bending vibration, and the antisymmetric C-O-C stretch mode of the β -1-4 glycosidic linkages associated with the linear xylose backbone of the AX, respectively [40,41]. The spectrum (b) in Figure 1 shows a characteristic band of amide I and amide II at the 1634 cm^{-1} and 1533 cm^{-1} signals, indicating the protein's presence [4,14,42,43]. The signals of amide I in the spectrum of the AXPP showed a shift to the left, and amide II showed a slight decrease in the band, which agrees with the reduction in protein content presented in Table 1. These results suggest that the partial removal of protein treatment causes these modifications to the protein bands. A previous study [14] reported a similar pattern in the sample spectrum, which was treated with protease. The bands at 3276 cm^{-1} and 2939 cm^{-1} correspond to the stretching of the OH and CH_2 groups, respectively, associated with the fingerprint region of polysaccharides related to the AX [24,44]. The findings from this study indicate that the enzymatic treatment does not alter the fingerprint of the AX, and only acts to modify its protein content.

3.2. AX and AXPP Covalent Cross-Linking

The rheological behavior of the AX and AXPP dispersions at 1% (w/v) treated with laccase as an oxidative agent is presented in Figure 3. The measurements were monitored via small-amplitude oscillatory shear, following the elastic modulus (G') and the viscous modulus (G''). The gelation kinetics after 90 min showed the typical behavior of AX dispersions exposed to laccase [12,22]. At the beginning of gelation, the AX and AXPP solutions rapidly increased the G' modulus, until they reached a plane region known as the plateau (Figure 3a). A higher G' value was observed for the AXPP (285 Pa) gel than for the AX (224 Pa) gel. These results indicate that the AXPP showed an increase of 27% in the G' value after enzymatic treatment. The crossover points of G' and G'' ($G' > G''$) were the same in the AX and AXPP gels (2 min). In a previous study [13], higher G' values were reported for DDGS AX gels before and after protease treatment (767 and 1291 Pa) at higher polysaccharide concentrations (2% w/v). This variance could be related to the AX

concentration of the gel. The mechanical spectrum of the AX and AXPP gels after 90 min of gelation are presented in Figure 3b, showing that the linear G' values are independent of the frequency over G'' , demonstrating the typical behavior of a solid gel. Similar results have been reported previously for DDGS AX gels [4,14,45].

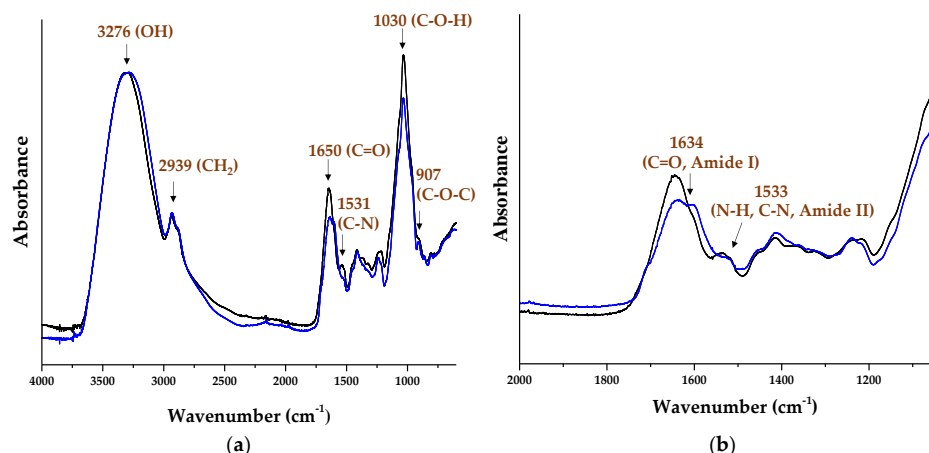


Figure 2. The FTIR spectra of (a) the AX (black line) and the AXPP (blue line); (b) the amide bands of the AX (black line) and the AXPP (blue line).

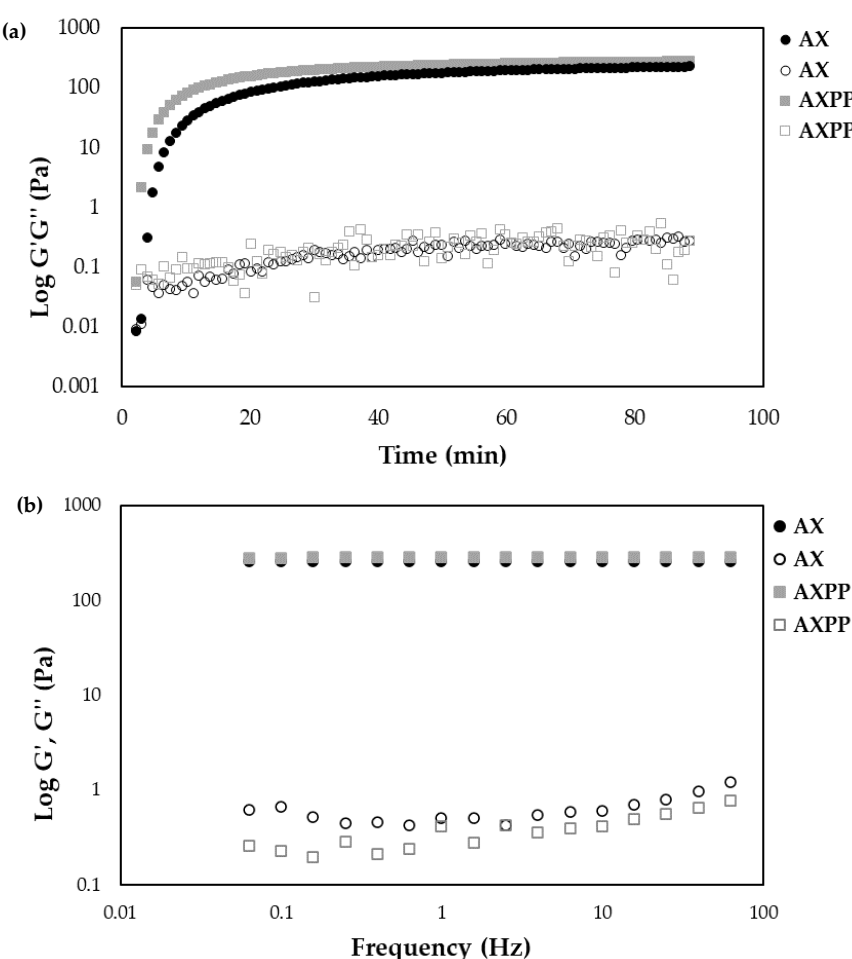


Figure 3. (a) The kinetics of gelation of the 1% dispersion (*w/v*) of AX and AXPP at 0.25 Hz and 5% strain; (b) the mechanical spectrum of the formed AX and AXPP gels at 5% strain at 25 °C. AX (G' ●; G'' ○); AXPP (G' ■; G'' □).

The di-FA and tri-FA were quantified after 90 min of gelation (Table 2), to examine the cross-linking content in the AX and AXPP gels. The di-FA of the AXPP gels presented a slight increase of 9%. The proportions of the 5-5', 8-O-4', and 8-5' structures were 10, 14, and 76% of the total di-FA detected in the AXPP gel. In AX gels, the proportions of the 5-5', 8-O-4', and 8-5' structures were 11, 15, and 74%, respectively. Furthermore, the di-FA/tri-FA ratio shows an approximate value of 5. This result suggests that the content of di-FAs in the gels is five times greater than that of tri-FAs. These findings imply that polysaccharide purification treatment does not significative affect the resulting covalent cross-linking content in the gels.

Table 2. The contents of dimers of FA (di-FAs) and trimers of FA (tri-FAs) in the AX and AXPP gels.

Gel	di-FA Structures			Total di-FAs	tri-FAs	di-FA/tri-FA Ratio
	5-5'	8-O-4'	8-5'			
AX	0.166 ± 0.027 ^a	0.218 ± 0.036 ^a	1.109 ± 0.162 ^a	1.49 ± 0.22 ^a	0.31 ± 0.05 ^a	4.82 ± 0.04 ^a
AXPP	0.161 ± 0.004 ^a	0.225 ± 0.007 ^a	1.246 ± 0.027 ^a	1.63 ± 0.04 ^a	0.31 ± 0.02 ^a	5.35 ± 0.50 ^a

The results are expressed in µg/mg of polysaccharide. The mean value of triplicate determinations ± SD. Values with similar letters in a column do not differ significantly ($p < 0.05$).

3.3. NAX and NAXPP Fabrication and Characteristics

The following morphological analyses were performed, to evaluate the differences between the NAX and NAXPP in a hydrated state. As shown in Table 3, the NAX and NAXPP particles presented different hydrodynamic diameters and zeta potential values. However, only the zeta potential value was statistically different. Figure 4a,c show the histogram associated with the size distribution of the observed dry particles (500 particles, determined via the program ImageJ). The range in nanoparticle size for the NAXs is 30–390 nm and, for the NAXPPs, it is 19–350 nm, and both samples showed a wide polydispersity. The enzymatic treatment of the AX led to a reduction in the particle size of the NAXPPs. Applying 1% phosphotungstic acid to the samples for negative staining creates a negative contrast, enabling the visualization of nanoparticles as bright objects against a dark background. The TEM micrographs (Figure 4b,d) revealed qualitative morphological variations in the particles, encompassing a spherical and regular shape and diverse sizes, and no agglomerates were observed in the NAXs and NAXPPs. The enzymatic treatment did not avoid the formation of NAXPPs. This shows that it is feasible to fabricate nanoparticles at low concentration (1%) with AXs and AXPPs. The reduction in protein content with the resulting structure modification favors the polysaccharide gelling capability, an increase in the elastic modulus (G'), and the formation of a more compact polymeric network, which could facilitate the fabrication of nanoparticles.

Table 3. The size and superficial charge of the NAXs and NAXPPs.

Parameter	NAX	NAXPP
Hydrodynamic diameter (nm)	328 ± 25 ^a	307 ± 46 ^a
Z potential (mV)	-30 ± 0.7 ^a	-27 ± 0.7 ^b

The mean value of triplicate determinations ± SD. Values with similar letters in a row do not differ significantly ($p < 0.05$).

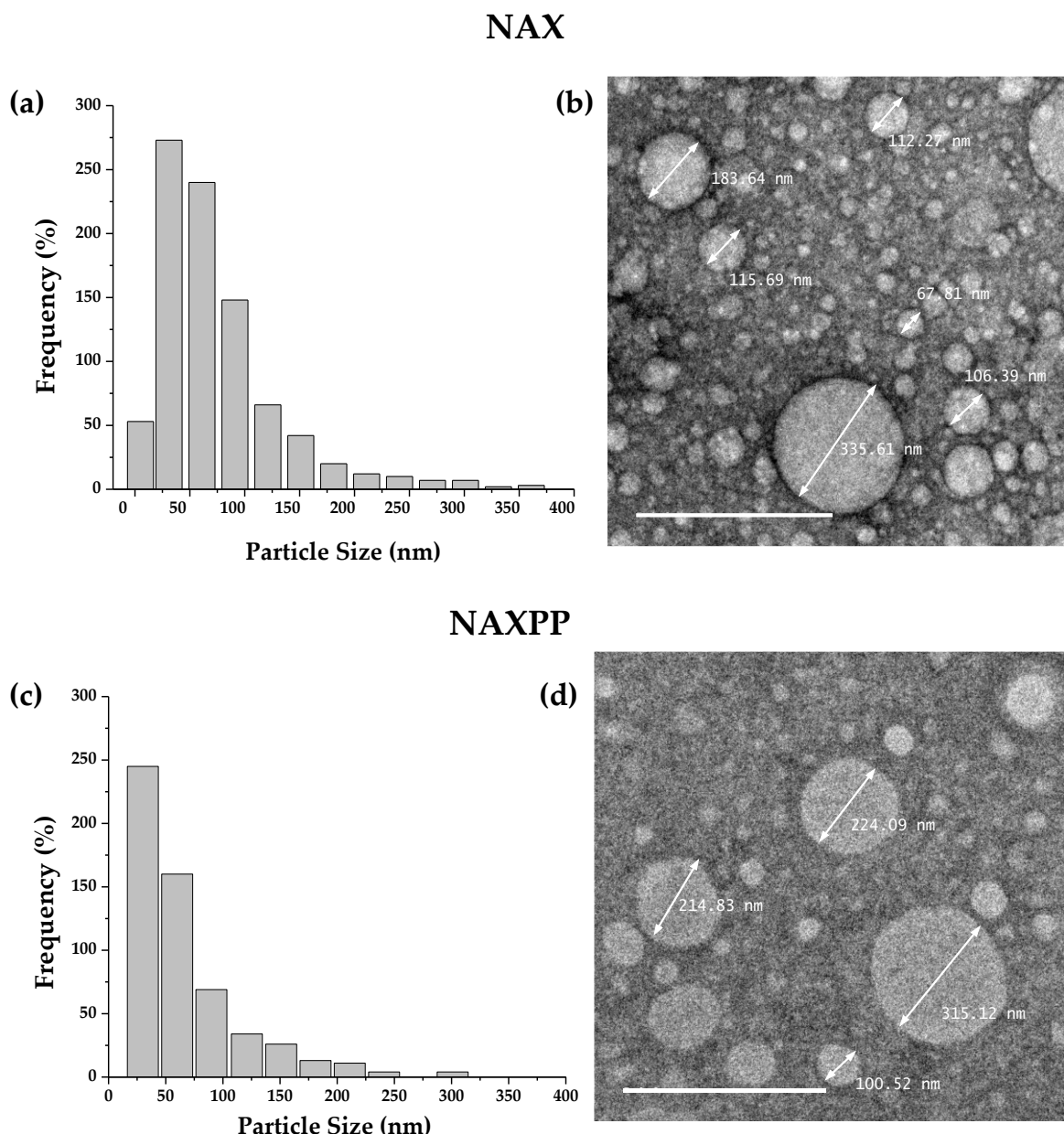


Figure 4. Particle size distribution histograms of NAXs and NAXPPs (**a,c**), and TEM micrographs of NAXs and NAXPPs (**b,d**).

3.4. CLSM Analysis of Gels and NAXs and NAXPPs

To examine the protein distribution in the AX network, confocal laser microscopy (CLSM) observations were analyzed for the AX and AXPP gels and the NAXs and NAXPPs. The CLSM analysis of the gels and nanoparticles samples (AX and AXPP 1% *w/v*) are shown in Figure 5. The red-highlighted areas in the images indicate the presence of protein, due to the fluorescent substance RITC, which can bind to proteins and emit this signal. The reduction in the luminous regions of the AXPP gels and nanoparticles is consistent with the decrease in their protein content, as previously reported [13].

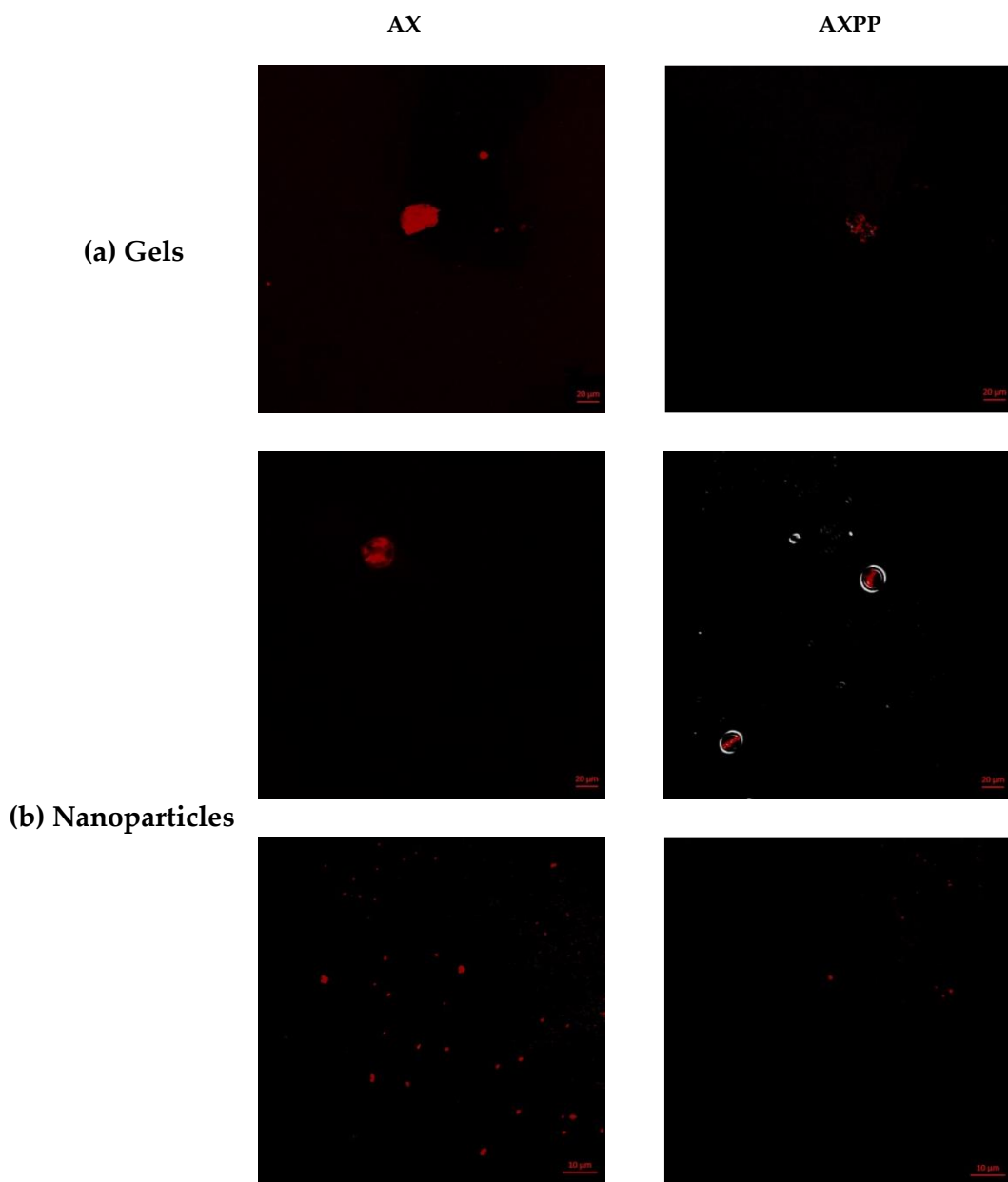


Figure 5. CLSM images of the AX and AXPP (a) gels (scale bar = 20 μ m), and (b) nanoparticles (NAXs and NAXPPs) (scale bar = 20 μ m and 10 μ m) at 1% with RITC at 0.02% (*w/v*).

4. Conclusions

Enzymatically treated arabinoxylans (AXPPs) registered a significant decrease in protein content and molecular weight, while no substantial changes in ferulic acid content and arabinose-to-xylose ratio were registered. AXPPs form gels with a significant increase in the storage modulus, in relation to AXs. AXs and AXPPs can form laccase-induced covalent electro-sprayed nanoparticles that present a spherical and regular morphology under transmission electron microscopy analysis. The nanoparticle diameter does not exhibit statistically significant differences between NAXs and NAXPPs. However, NAXPPs show a significant reduction in zeta potential value compared to NAXs. The protein distribution was observed via CLSM, and showed how the AXPPs presented a reduction in luminous areas. The development of nanoparticles based on enzymatically treated AXs may represent an opportunity to design biomaterials with potential pharmaceutical and biomedical applications, due to this polysaccharide's biocompatibility and biodegradability characteristics.

Author Contributions: Y.D.A.-F. and E.C.-M. designed the experiments; A.R.-C., J.L.-M., J.T.-C. and A.L.M.-L. are coauthors, and assisted in the research, providing supervision, the revision of the manuscript, software use, reagents, materials, and laboratory equipment. All authors have read and agreed to the published version of the manuscript.

Funding: This research was funded by Consejo Nacional de Humanidades, Ciencias y Tecnologías (CONAHCYT): CONAHCYT INFR-2014-01-226082. Yubia De Anda-Flores thanks CONAHCYT for the postdoctoral fellowship (Modalidad Estancia Posdoctoral Académica Inicial 2022-Convocatoria Estancias Posdoctorales por México 2022).

Institutional Review Board Statement: Not applicable.

Data Availability Statement: The data presented in this study are available on request from the corresponding author. The data are not publicly available due to a patent application in process.

Acknowledgments: The authors are pleased to acknowledge Alma C. Campa Mada and Karla G. Martínez Robinson for technical laboratory support and writing support. To J. Alfonso Sánchez Villegas for technical support in the laboratory with using the electro-spray system, and to Eduardo A. Larios for transmission electron microscopy (TEM) analysis. The TEM experiments were performed at the TEM Laboratory of the University of Sonora. The authors are grateful to Humberto Astiazaran-Garcia and Bertha I Pacheco-Moreno for their assistance in microscopy analysis at the C2+ Confocal Microscope System.

Conflicts of Interest: The authors declare no conflict of interest.

References

1. Saulnier, L.; Guillon, F.; Sado, P.-E.; Chateigner-Boutin, A.-L.; Rouau, X. Plant Cell Wall Polysaccharides in Storage Organs: Xylans (Food Applications). In *Reference Module in Chemistry, Molecular Sciences and Chemical Engineering*; Elsevier: Amsterdam, The Netherlands, 2013; pp. 653–689. ISBN 978-0-12-409547-2.
2. Izidorczyk, M.; Biliaderis, C.G.; Bushuk, W. Comparison of the structure and composition of water-soluble pentosans from different wheat varieties. *Cereal Chem.* **1991**, *68*, 139–144.
3. Mendez-Encinas, M.A.; Carvajal-Millan, E.; Rascon-Chu, A.; Astiazaran-Garcia, H.F.; Valencia-Rivera, D.E. Ferulated Arabinoxylans and Their Gels: Functional Properties and Potential Application as Antioxidant and Anticancer Agent. *Oxid. Med. Cell. Longev.* **2018**, *2018*, 2314759. [[CrossRef](#)]
4. Marquez-Escalante, J.A.; Carvajal-Millan, E. Feruloylated Arabinoxylans from Maize Distiller’s Dried Grains with Solubles: Effect of Feruloyl Esterase on their Macromolecular Characteristics, Gelling, and Antioxidant Properties. *Sustainability* **2019**, *11*, 6449. [[CrossRef](#)]
5. Roth, M.; Jekle, M.; Becker, T. Opportunities for upcycling cereal byproducts with special focus on Distiller’s grains. *Trends Food Sci. Technol.* **2019**, *91*, 282–293. [[CrossRef](#)]
6. Izidorczyk, M.S.; Biliaderis, C.G. Cereal arabinoxylans: Advances in structure and physicochemical properties. *Carbohydr. Polym.* **1995**, *28*, 33–48. [[CrossRef](#)]
7. Morales-Ortega, A.; Niño-Medina, G.; Carvajal-Millán, E.; Gardea-Béjar, A.; Torres-Chávez, P.; López-Franco, Y.; Rascón-Chu, A.; Lizardi-Mendoza, J. Los Arabinoxilanos Ferulados De Cereales. Una Revisión De Sus. *Rev. Fitotec. Mex.* **2013**, *36*, 439–446.
8. Saulnier, L.; Crépeau, M.J.; Lahaye, M.; Thibault, J.F.; Garcia-Conesa, M.T.; Kroon, P.A.; Williamson, G. Isolation and structural determination of two 5,5'-diferuloyl oligosaccharides indicate that maize heteroxylans are covalently cross-linked by oxidatively coupled ferulates. *Carbohydr. Res.* **1999**, *320*, 82–92. [[CrossRef](#)]
9. Saulnier, L.; Marot, C.; Chanliaud, E.; Thibault, J.F. Cell wall polysaccharide interactions in maize bran. *Carbohydr. Polym.* **1995**, *26*, 279–287. [[CrossRef](#)]
10. Carvajal-Millan, E.; Landillon, V.; Morel, M.-H.; Rouau, X.; Doublier, J.-L.; Micard, V. Arabinoxylan gels: Impact of the feruloylation degree on their structure and properties. *Biomacromolecules* **2005**, *6*, 309–317. [[CrossRef](#)]
11. Martínez-López, A.L.; Carvajal-Millan, E.; Marquez-Escalante, J.; Campa-Mada, A.C.; Rascón-Chu, A.; López-Franco, Y.L.; Lizardi-Mendoza, J. Enzymatic cross-linking of ferulated arabinoxylan: Effect of laccase or peroxidase catalysis on the gel characteristics. *Food Sci. Biotechnol.* **2019**, *28*, 311–318. [[CrossRef](#)]
12. Carvajal-Millan, E.; Rascón-Chu, A.; Márquez-Escalante, J.A.; Micard, V.; de León, N.P.; Gardea, A. Maize bran gum: Extraction, characterization and functional properties. *Carbohydr. Polym.* **2007**, *69*, 280–285. [[CrossRef](#)]
13. Mendez-Encinas, M.A.; Carvajal-Millan, E.; Yadav, M.P.; López-Franco, Y.L.; Rascon-Chu, A.; Lizardi-Mendoza, J.; Brown-Bojorquez, F.; Silva-Campa, E.; Pedroza-Montero, M. Partial removal of protein associated with arabinoxylans: Impact on the viscoelasticity, crosslinking content, and microstructure of the gels formed. *J. Appl. Polym. Sci.* **2019**, *136*, 47300. [[CrossRef](#)]
14. Yadav, M.P.; Fishman, M.L.; Chau, H.K.; Johnston, D.B.; Hicks, K.B. Molecular Characteristics of Corn Fiber Gum and Their Influence on CFG Emulsifying Properties. *Cereal Chem. J.* **2007**, *84*, 175–180. [[CrossRef](#)]
15. Yadav, M.P.; Nuñez, A.; Hicks, K.B. Isolation, Purification, and Identification of Protein Associated with Corn Fiber Gum. *J. Agric. Food Chem.* **2011**, *59*, 13289–13294. [[CrossRef](#)]

16. Fincher, G.; Stone, B. A Water-soluble Arabinogalactan-Peptide From Wheat Endosperm. *Aust. J. Biol. Sci.* **1974**, *27*, 117–132. [[CrossRef](#)]
17. Yadav, M.P.; Cooke, P.; Johnston, D.B.; Hicks, K.B. Importance of Protein-Rich Components in Emulsifying Properties of Corn Fiber Gum. *Cereal Chem. J.* **2010**, *87*, 89–94. [[CrossRef](#)]
18. Rudjito, R.C.; Ruthes, A.C.; Jiménez-Quero, A.; Vilaplana, F. Feruloylated arabinoxylans from wheat bran: Optimization of extraction process and validation at pilot scale. *ACS Sustain. Chem. Eng.* **2019**, *7*, 13167–13177. [[CrossRef](#)]
19. Paesani, C.; Degano, A.L.; Ines, Z.; Zalosnik, M.I.; Fabi, J.P.; Pérez, G.T. Enzymatic modification of arabinoxylans from soft and hard Argentinian wheat inhibits the viability of HCT-116 cells. *Food Res. Int.* **2021**, *147*, 110466. [[CrossRef](#)]
20. Tavano, O.L.; Berenguer-Murcia, A.; Secundo, F.; Fernandez-Lafuente, R. Biotechnological Applications of Proteases in Food Technology. *Compr. Rev. Food Sci. Food Saf.* **2018**, *17*, 412–436. [[CrossRef](#)]
21. Méndez-Encinas, M.; Carvajal-Millan, E.; Yadav, M.; Valenzuela-Soto, E.M.; Figueroa-Soto, C.G.; Tortoledo-Ortiz, O.; García-Sánchez, G. Gels of ferulated arabinoxylans: Rheology, structural parameters and microstructure. In *Advances in Physicochemical Properties of Biopolymers*; Bentham Science Publishers: Beijing, China, 2017; pp. 208–221.
22. Méndez-Encinas, M.; Carvajal-Millan, E.; Rascón-Chu, A.; López-Franco, Y.; Lizardi, J. Arabinoxilan y la Relación de la Fracción Proteica Remanente con la Capacidad Gelificante del Polisacárido. *Acta Univ.* **2019**, *29*, e1755. [[CrossRef](#)]
23. González-Estrada, R.; Calderón-Santoyo, M.; Carvajal-Millan, E.; De Jesús Ascencio Valle, F.; Ragazzo-Sánchez, J.A.; Brown-Bojorquez, F.; Rascón-Chu, A. Covalently cross-linked arabinoxylans films for Debaryomyces hansenii entrapment. *Molecules* **2015**, *20*, 11373–11386. [[CrossRef](#)]
24. Paz-Samaniego, R.; Rascón-Chu, A.; Brown-Bojorquez, F.; Carvajal-Millan, E.; Pedroza-Montero, M.; Silva-Campa, E.; Sotelo-Cruz, N.; López-Franco, Y.L.; Lizardi-Mendoza, J. Electrospray-assisted fabrication of core-shell arabinoxylan gel particles for insulin and probiotics entrapment. *J. Appl. Polym. Sci.* **2018**, *135*, 46411. [[CrossRef](#)]
25. Morales-Burgos, A.M.; Carvajal-Millan, E.; Rascón-Chu, A.; Martínez-López, A.L.; Lizardi-Mendoza, J.; López-Franco, Y.L.; Brown-Bojorquez, F. Tailoring reversible insulin aggregates loaded in electrosprayed arabinoxylan microspheres intended for colon-targeted delivery. *J. Appl. Polym. Sci.* **2019**, *136*, 47960. [[CrossRef](#)]
26. Ohlmaier-Delgadillo, F.; Carvajal-Millan, E.; López-Franco, Y.L.; Islas-Osuna, M.A.; Micard, V.; Antoine-Assor, C.; Rascón-Chu, A. Ferulated Pectins and Ferulated Arabinoxylans Mixed Gel for *Saccharomyces boulardii* Entrapment in Electrosprayed Microbeads. *Molecules* **2021**, *26*, 2478. [[CrossRef](#)]
27. Seidi, F.; Jenjob, R.; Phakkeeree, T.; Crespy, D. Saccharides, oligosaccharides, and polysaccharides nanoparticles for biomedical applications. *J. Control. Release* **2018**, *284*, 188–212. [[CrossRef](#)] [[PubMed](#)]
28. Jacob, J.; Haponiuk, J.T.; Thomas, S.; Gopi, S. Biopolymer based nanomaterials in drug delivery systems: A review. *Mater. Today Chem.* **2018**, *9*, 43–55. [[CrossRef](#)]
29. De Anda-Flores, Y.; Carvajal-Millan, E.; Lizardi-Mendoza, J.; Rascon-Chu, A.; Martínez-López, A.L.; Marquez-Escalante, J.; Brown-Bojorquez, F.; Tanori-Cordova, J. Covalently Cross-Linked Nanoparticles Based on Ferulated Arabinoxylans Recovered from a Distiller’s Dried Grains Byproduct. *Processes* **2020**, *8*, 691. [[CrossRef](#)]
30. De Anda-Flores, Y.; Carvajal-Millan, E.; Lizardi-Mendoza, J.; Rascon-Chu, A.; Tanori-Cordova, J.; Martínez-López, A.L.; Burgara-Estrella, A.J.; Pedroza-Montero, M.R. Conformational Behavior, Topographical Features, and Antioxidant Activity of Partly De-Esterified Arabinoxylans. *Polymers* **2021**, *13*, 2794. [[CrossRef](#)]
31. Vansteenkiste, E.; Babot, C.; Rouau, X.; Micard, V. Oxidative gelation of feruloylated arabinoxylan as affected by protein. Influence on protein enzymatic hydrolysis. *Food Hydrocoll.* **2004**, *18*, 557–564. [[CrossRef](#)]
32. Bradford, M.M.; Pedroche, J.; Yust, M.M.; Girón-Calle, J.; Alaiz, M.; Millán, F.; Vioque, J. A Rapid and Sensitive Method for the Quantitation of Microgram Quantities of Protein Utilizing the Principle of Protein-Dye Binding. *Anal. Biochem.* **1976**, *72*, 248–254. [[CrossRef](#)]
33. Dervilly-Pinel, G.; Thibault, J.-F.; Saulnier, L. Experimental evidence for a semi-flexible conformation for arabinoxylans. *Carbohydr. Res.* **2001**, *330*, 365–372. [[CrossRef](#)]
34. Rascón-Chu, A.; Díaz-Baca, J.A.; Carvajal-Millan, E.; Pérez-López, E.; Hotchkiss, A.T.; González-Ríos, H.; Balandrán-Quintana, R.; Campa-Mada, A.C. Electrosprayed core-shell composite microbeads based on pectin-arabinoxylans for insulin carrying: Aggregation and size dispersion control. *Polymers* **2018**, *10*, 108. [[CrossRef](#)]
35. Rochín-Wong, S.; Rosas-Durazo, A.; Zavala-Rivera, P.; Maldonado, A.; Martínez-Barbosa, M.; Vélaz, I.; Tánori, J. Drug Release Properties of Diflunisal from Layer-By-Layer Self-Assembled κ-Carrageenan/Chitosan Nanocapsules: Effect of Deposited Layers. *Polymers* **2018**, *10*, 760. [[CrossRef](#)]
36. Keeratiburana, T.; Hansen, A.R.; Soontaranon, S.; Blennow, A.; Tongta, S. Porous high amylose rice starch modified by amyloglucosidase and maltogenic α-amylase. *Carbohydr. Polym.* **2020**, *230*, 115611. [[CrossRef](#)]
37. Al-Assaf, S.; Sakata, M.; McKenna, C.; Aoki, H.; Phillips, G.O. Molecular associations in acacia gums. *Struct. Chem.* **2009**, *mboxemph20*, 325–336. [[CrossRef](#)]
38. Iravani, S.; Fitchett, C.S.; Georget, D.M.R. Physical characterization of arabinoxylan powder and its hydrogel containing a methyl xanthine. *Carbohydr. Polym.* **2011**, *85*, 201–207. [[CrossRef](#)]
39. Kačuráková, M.; Ebringerová, A.; Hirsch, J.; Hromádková, Z. Infrared study of arabinoxylans. *J. Sci. Food Agric.* **1994**, *66*, 423–427. [[CrossRef](#)]

40. Kacuráková, M. FT-IR study of plant cell wall model compounds: Pectic polysaccharides and hemicelluloses. *Carbohydr. Polym.* **2000**, *43*, 195–203. [[CrossRef](#)]
41. Morales-Ortega, A.; Carvajal-Millan, E.; López-Franco, Y.; Rascón-Chu, A.; Lizardi-Mendoza, J.; Torres-Chavez, P.; Campa-Mada, A. Characterization of Water Extractable Arabinoxylans from a Spring Wheat Flour: Rheological Properties and Microstructure. *Molecules* **2013**, *18*, 8417–8428. [[CrossRef](#)]
42. Sárossy, Z.; Tenkanen, M.; Pitkänen, L.; Bjerre, A.-B.; Plackett, D. Extraction and chemical characterization of rye arabinoxylan and the effect of β -glucan on the mechanical and barrier properties of cast arabinoxylan films. *Food Hydrocoll.* **2013**, *30*, 206–216. [[CrossRef](#)]
43. Sene, C.; McCann, M.C.; Wilson, R.H.; Grinter, R. Fourier-Transform Raman and Fourier-Transform Infrared Spectroscopy (An Investigation of Five Higher Plant Cell Walls and Their Components). *Plant Physiol.* **1994**, *106*, 1623–1631. [[CrossRef](#)] [[PubMed](#)]
44. Robert, P.; Marquis, M.; Barron, C.; Guillon, F.; Saulnier, L. FT-IR investigation of cell wall polysaccharides from cereal grains. Arabinoxylan infrared assignment. *J. Agric. Food Chem.* **2005**, *53*, 7014–7018. [[CrossRef](#)] [[PubMed](#)]
45. Mendez-Encinas, M.A.; Carvajal-Millan, E.; Rascón-Chu, A.; Astiazarán-García, H.; Valencia-Rivera, D.E.; Brown-Bojorquez, F.; Alday, E.; Velazquez, C. Arabinoxylan-Based Particles: In Vitro Antioxidant Capacity and Cytotoxicity on a Human Colon Cell Line. *Medicina* **2019**, *55*, 349. [[CrossRef](#)] [[PubMed](#)]

Disclaimer/Publisher's Note: The statements, opinions and data contained in all publications are solely those of the individual author(s) and contributor(s) and not of MDPI and/or the editor(s). MDPI and/or the editor(s) disclaim responsibility for any injury to people or property resulting from any ideas, methods, instructions or products referred to in the content.